Applied Thermal Engineering 234 (2023) 121197

Contents lists available at ScienceDirect

Applied Thermal Engineering

journal homepage: www.elsevier.com/locate/ate

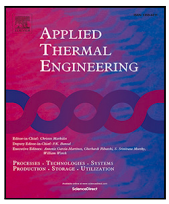

Research Paper

The thermodynamic potential of high-temperature transcritical heat pump cycles for industrial processes with large temperature glides

Elias Vieren [a,*], Toon Demeester [a], Wim Beyne [a], Alessia Arteconi [b,c,d], Michel De Paepe [a,e], Steven Lecompte [a,e]

[a] Ghent University, Department of Electromechanical, Systems and Metal Engineering, Sint-Pietersnieuwstraat 41, 9000 Gent, Belgium
[b] KU Leuven, Department of Mechanical Engineering, Leuven, 3000, Belgium
[c] EnergyVille, 3600, Genk, Belgium
[d] Dipartimento di Ingegneria Industriale e Scienze Matematiche, Università Politecnica delle Marche, 60131, Ancona, Italy
[e] FlandersMake@UGent – Core lab EEDT - MP, Leuven, Belgium

ARTICLE INFO

Keywords:
High-temperature heat pump
Transcritical cycles
Industrial heat pump
Temperature glide
Drying

ABSTRACT

Industrial heat pumps up to 200 °C are an emerging technology with the potential to reshape the industrial heating supply. For large heat sink temperature glides, transcritical cycles are able to increase the power-to-heat efficiency. Its potential is however yet to be unlocked. To examine this potential, a thermodynamic optimization model is proposed. The model includes robust cycle optimization, is able to screen a large set of working fluids, and includes proper post-processing. This model is applied to three highly relevant industrial cases, namely thermal oil heating, superheated steam drying and spray drying. The heat sink temperature glides for the respective case studies are 60 K, 81 K and 105 K. The results show that a temperature glide larger than 60 K is desired to achieve a better coefficient of performance (COP) with transcritical cycles compared to the classical subcritical cycles. Moreover, potential working fluids were identified for these high operational temperatures. For the case study with a heat sink temperature glide of 81 K, transcritical cycles allowed for a COP increase of 4.6%, whereas this increased to 7.3% for a heat sink temperature glide of 105 K. Furthermore, transcritical cycles introduce a much larger volumetric heating capacity, a lower compressor discharge temperature and a substantially lower pressure ratio. In addition, the best performing working fluids for subcritical cycles are highly flammable, which is only the case for some transcritical working fluids. Therefore, these cycles can be beneficial for temperature glides below 60 K. The compressor for transcritical cycles should however be able to cope with pressures up to 60 bar. If these compressors are available, transcritical cycles are shown to be superior compared to classical subcritical cycles.

1. Introduction

The industrial heating sector is dominated by the combustion of fossil fuels [1]. These fossil fuels have significant contributions in the current greenhouse gas (GHG) emissions [1]. Moreover, fossil fuel prices are highly unpredictable. Renewable electricity on the other hand, which is less dependent on geopolitical aspects, has an overall decreasing price trend. Therefore, vapor compression high-temperature heat pumps (HTHPs) are being proposed for industrial heat supply up until 200 °C [2]. An overview of the operating principles, refrigerants, application potential and challenges of HTHPs can be found in recent review articles [3–6]. These HTHP are becoming cost-effective technologies compared to fossil fuel combustion [7,8]. Moreover, due to their high power-to-heat efficiency, HTHPs allow for a significant reduction in GHG emissions, even under the current European energy mix [9]. Further enhancing the performance of HTHPs would allow for improved cost-efficiencies and lower GHG emissions, increasing the adoption rate of the technology.

One way to increase the performance of HTHPs is by reducing exergy losses in the heat exchangers. Knowing that heat transfer is a main source of exergy destruction in HTHPs [10]. This exergy destruction can be minimized by closely matching the temperature profile of refrigerant and secondary medium.

In transcritical heat pump cycles, heat rejection happens at pressures above the critical pressure. Therefore, compared to classical subcritical operation, these cycles are able to provide a better temperature match in scenarios of large heat sink temperature glides as shown in Fig. 1.

* Corresponding author.
E-mail address: elias.vieren@ugent.be (E. Vieren).

https://doi.org/10.1016/j.applthermaleng.2023.121197
Received 18 November 2022; Received in revised form 10 July 2023; Accepted 17 July 2023
Available online 24 July 2023

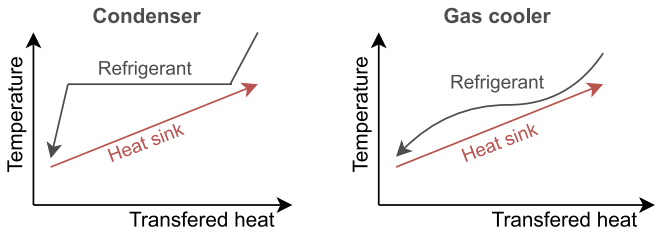

Fig. 1. Temperature profile during heat rejection for subcritical operation (condenser) and transcritical or supercritical operation (gas cooler).

Another well-suited method to reduce exergy destruction is by using zeotropic mixtures, which are studied both for HTHPs [11–14] as for organic Rankine cycles (ORCs) [15,16]. Zeotropic mixtures experience a temperature glide during phase change which can be matched with the temperature glide of the heat source or sink. However, obtaining large temperature glides with zeotropic mixtures poses a risk for fractionation [17,18].

This study focuses on large temperature glides at the heat sink side, which are common in industrial applications such as drying (e.g. spray drying or superheated steam drying), thermal oil heating, pressurized hot water production, air preheating or fluid (pre)heating. For these applications, use of zeotropic mixtures may be less interesting because of the risk of fractionation. Furthermore, the strongly different temperature glides of the heat source and sink may severely limit the obtainable efficiency gain of zeotropic mixtures. Transcritical cycles however, are well suited for these types of temperature glides.

The transcritical vapor compression cycle was proposed by Lorentzen in 1990 [19], who identified CO2 as a near-ideal refrigerant [20]. Since the publication by Lorentzen [19] much research has been performed on transcritical CO2 cycles; an overview of transcritical CO2 heat pumps and their relevance can be found in several review articles [21–24]. CO2 however has a low critical temperature of 31 °C and a high critical pressure of 73.6 bar. Consequently, pressures in CO2 systems are typically 5–10 times higher compared to other refrigerants [25]. This may cause several challenges in component design and safety concerns, especially when high operational temperatures are targeted [25]. Moreover, to keep heat transfer at the heat source in the two-phase region, low temperatures are required at the evaporator side (25–30 °C) [26]. Therefore, its use in high-temperature applications is commonly limited to heat sinks with outlet temperatures of 120 °C and considerably lower heat sink inlet temperatures [4,27].

Whereas transcritical operation is common practice for CO2 heat pump cycles, few transcritical HTHPs are found operating with other refrigerants. Besbes et al. [28] constructed a 30 kW_{th} transcritical heat pump prototype with R32 as refrigerant, to be implemented in drying plants. In the set-up, air was heated from 60 to 120 °C, with effluents available at 50 °C. A COP of 3.69 was observed, which corresponds to an exergy efficiency of 63%. Chahla et al. [29] adapted the set-up constructed by Besbes et al. [28] for use of Hydrofluro-Olefins (HFOs) as refrigerant. In their work, air heating at 90 °C or 100 °C to 150 °C is experimentally investigated, using effluents at 82 °C. The adapted heat pump reached COPs up to 3.72. Kimura et al. [30] developed a transcritical butane (R600) HTHP with as goal to raise the temperature of thermal oil from 80 to 180 °C, employing a hot water heat source at 80 °C. The targeted COP is 3.5. Newly designed oil-free centrifugal compressors with active magnetic bearings were used. The heat pump system has a capacity of 300 kW_{th}. Verdnik and Rieberer [31], designed a single-stage HTHP prototype with a suction-gas-cooled reciprocating compressor, low pressure suction accumulator and internal heat exchanger (IHX), also using R600 as refrigerant. Transcritical operation enabled to raise the temperature of the heat sink from 80 °C to 160 °C. A COP of 3.1 and a heating capacity of 24.2 kW_{th} was achieved with a heat source cooled from 60 °C to 55 °C. Moreover, the influence of the discharge pressure and suction gas superheat in the IHX on the COP and heating capacity was studied.

Whereas some experimental research is performed on transcritical industrial heat pumps with refrigerants other than CO2, few working fluid screenings are performed and few relevant applications for transcritical HTHPs up to 200 °C are presented. Sarkar et al. [27] considered subcritical and transcritical cycles for, amongst others, a generic case study with heat sink outlet temperatures up to 200 °C, but only considered four refrigerants (i.e. carbon dioxide, ammonia, propane and isobutane). Wang et al. [32] compared subcritical and transcritical heat pump cycles for spray dryers operating at 200 °C, where most refrigerants in Engineering Equation Solver (EES) were assessed. However, due to the lack of a heat source with a suitable energy content, the heat sink outlet temperatures were limited to 110 °C. For this the high global warming potential (GWP) refrigerant R134a was proposed as most promising, with R32 and R290 also showing good energy efficiency. Arpagaus et al. [33], modeled a transcritical heat pump cycle with and without IHX and a transcritical heat pump cycle with parallel compression. With the use of the model two case studies are considered, namely, air heating from 30 to 200 °C with a hot water heat source at 80 °C, and water heating from 100 to 200 °C with use of moist air at 30 °C as heat source. The investigated working fluids were R245fa, four low-GWP HFOs and the hydrocarbons R601 and R600. The results show that the cycle with IHX has the highest performance and lowest discharge pressure. Moreover, this cycle is convenient to control. The results also showed that the gas cooler pressure has a large impact on the COP.

In conclusion, it is unclear for transcritical HTHPs what the technology potential is for high temperature needs (up to 200 °C), how these HTHPs should be optimally designed and what further challenges remain. In this work, three relevant industrial case studies, with different temperature glides, are proposed as a starting ground. The need to analyze different temperature profiles is also emphasized by Arpagaus et al. [33], who suggest that future research into transcritical cycles should include more temperature conditions. By doing so it can be determined for which boundary conditions (i.e. applications) transcritical operation becomes more beneficial than classical subcritical operation. Moreover, suitable working fluids for transcritical or subcritical operation can be identified for the targeted applications, since all working fluids within REFPROP 10.0 [34] are considered in this work. This is also stressed in the recent review paper of Adamson et al. [6] on transcritical heat pump cycles, which state that one of the challenges is: 'The identification of efficient refrigerants (or refrigerant blends), beyond CO2, to maximize COP for specific applications while keeping within pressure limits'. In addition, suitable working fluids will be presented for heat pump supply temperatures up to 200 °C in general, which is scarcely studied in the literature. Furthermore, this study considers and compares the influence of flammability and the use of an internal heat exchanger for the different case studies.

2. Methods

To demonstrate when transcritical cycles are relevant, an optimization model is developed. The model differentiates from most models reported in the literature [35–38] in the sense that it includes a robust optimization algorithm. This algorithm optimizes, amongst others, the pressure during heat delivery and the amount of subcooling. Both parameters have a large influence on the COP for transcritical, or near-transcritical, cycles [27,31]. Moreover, an optimized subcooling also has a strong impact on the COP for subcritical cycles when used for applications with large temperature glides [39]. The model also optimizes the pressure during heat extraction and the amount of superheat, and covers a wet compression detection. Furthermore, it includes a proper post-processing so that only working fluids are reported that are practically relevant.

The basis of the optimization model is the thermodynamic model, which takes the industrial application (i.e. boundary conditions) and the heat pump operating conditions as input as shown in Fig. 2. On top of this thermodynamic model a global optimizer maximizes the COP by varying the heat pump operating conditions. In order to find a technically feasible solution, several optimization constraints are applied to the global optimizer. The optimization is performed on a large set of working fluids. This set is obtained starting from the REFPROP 10.0 database of pure working fluids [34] subjected to a first fluid screening step. Once all optimal operating conditions and cycle variables are determined for each working fluid, post-processing is performed on these intermediate results by applying technical constraints, which eventually leads to the reported results in this work. In what follows each of the steps in the methodology are explained in detail.

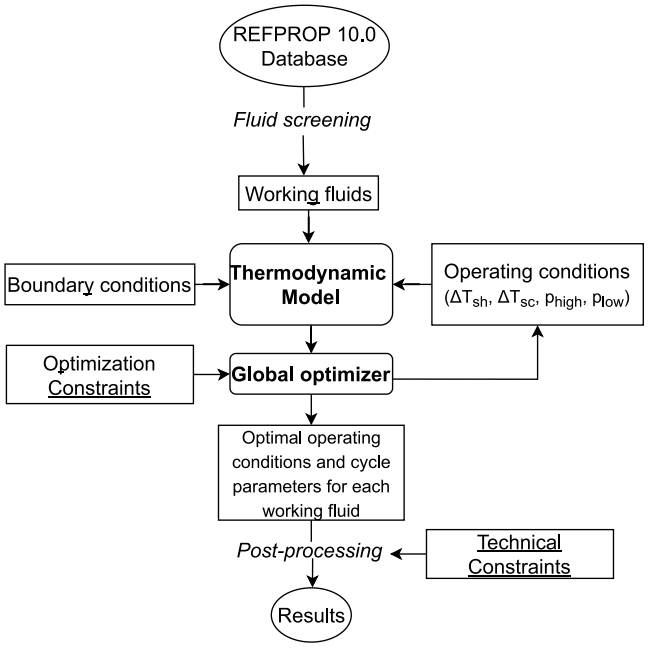

Fig. 2. Flowchart of the optimization model.

2.1. Thermodynamic model

In order to estimate the performance, a thermodynamic model in Python is developed. The model simulates a heat pump cycle which consists of a compressor, evaporator, condenser/gas cooler, expansion valve and optionally an IHX as shown in Fig. 3. In this figure a number, or letter, for each state is given. These numbers, or letters, will be used throughout this work to indicate the respective states. Depending on the case study, more complex cycles could be beneficial to increase the performance of the heat pump. However, it was not included in the scope of this work. In the literature transcritical operation is seen as a solution to increase performance without adding additional components to the cycle.

The input parameters of the thermodynamic model are: heat sink inlet and outlet state, heat sink mass flow rate, heat pump operating conditions, the inlet state of the heat source and the mass flow rate of the heat source. Note that the heat sink is completely defined a priori, in contrast to the heat source outlet state, which is a function of the COP and the amount of heat supplied.

The heat pump operating conditions variables are: pressure during heat extraction (p_{low}) and delivery (p_{high}), amount of superheat (ΔT_{sh}) and amount of subcooling (ΔT_{sc}). For operation above the critical point (i.e. transcritical operation), subcooling is defined with respect to the critical point. Consequently, according to this definition, the subcooling can have a negative or positive sign. The different components of the heat pump cycle are modeled as described in the upcoming sections.

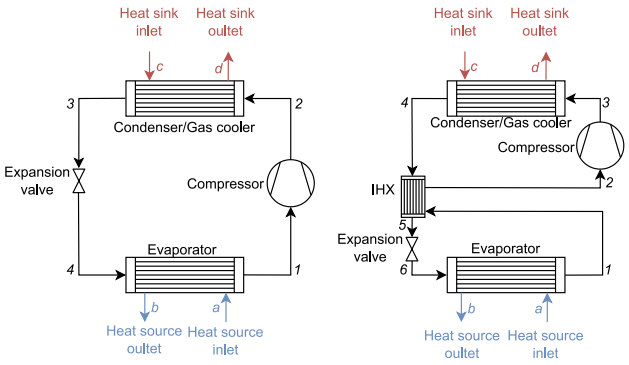

Fig. 3. Single-stage heat pump cycle, without and with IHX.

2.1.1. Compressor model

The compressor is modeled by considering a fixed isentropic efficiency (η_{is}) of 75% [4,40] and a volumetric efficiency (η_{vol}) of 90% [41]. Mateu-Royo et al. [42] constructed a prototype HTHP using R245fa as the refrigerant. They performed an energy and exergy analysis for heat source temperatures between 60 and 80 °C, and heat sink temperatures between 90 and 140 °C. The results showed an isentropic efficiency varying between from just under 70% to somewhat over 80%. Furthermore, volumetric efficiencies ranging from around 87% to almost 100% were observed. This justifies the use of the selected isentropic and volumetric efficiencies from the literature. Whereas more advanced models exist that estimate these efficiencies based upon the operating conditions and/or fluid properties, these are always developed for a specific compressor type and are only valid within a certain range of volume flow rates [43–45]. In order to have a generally valid compressor model, fixed efficiencies are used. The power use of the compressor ($\dot{W}_{comp}$) is calculated as the product of the working fluid mass flow rate ($\dot{m}_{wf}$) and the enthalpy difference over the compressor as shown in Eq. (1):

$$\dot{W}_{comp} = \dot{m}_{wf} \cdot (h_{comp,out} - h_{comp,in}) \tag{1}$$

The enthalpy at the compressor outlet ($h_{comp,out}$) is calculated based on the enthalpy at the inlet of the compressor ($h_{comp,in}$) and the considered isentropic efficiency. An ideal mechanical and drive efficiency is considered to convert the corresponding power to the electrical power.

Depending on the shape of the vapor saturation curve, a working fluid for use in heat pumps can be categorized as: dry fluid ($dT/ds < 0$), wet fluid ($dT/ds > 0$) or isentropic fluid ($dT/ds = \infty$). A working fluid is classified as 'wet' when an isentropic compression, starting from saturated vapor, goes through the two-phase region. When the compressor is not designed to handle two-phase compression, a certain amount of superheat is required for wet fluids [45]. Another option to avoid wet compression is employing an IHX [46]. Within the developed model, the occurrence of two-phase compression is monitored and the superheat is increased if necessary to avoid wet compression.

2.1.2. Heat exchanger model

Underwood [47] suggests that in close-coupled packaged plants, the pressure losses of the refrigerant during heat exchange can be disregarded since they are typically insignificant. Therefore, pressure drops are not considered. Furthermore, the heat exchanger losses to the environment are set to zero. In the literature [45,48–51] it is also observed that both losses are commonly set to zero, due to their minimal effects. Therefore, the heat transfer rate is calculated by multiplying the mass flow rate of the medium ($\dot{m}$) with the absolute value of difference in enthalpy at the heat exchanger inlet (h_{in}) and outlet (h_{out}) as shown in Eq. (2):

$$\dot{m}_{wf} \cdot |h_{wf,in} - h_{wf,out}| = \dot{m}_{sf} \cdot |h_{sf,in} - h_{sf,out}| \tag{2}$$

where the subscript "wf" refers to "working fluid" and the subscript "sf" refers to "secondary fluid". The evaporator and condenser/gas cooler are sized assuming a theoretical limiting case by setting a predetermined pinch point temperature difference (PPTD), and the outlet states are defined by the imposed superheat or subcooling. It should be noted, however, that with a suitable temperature match between refrigerant and heat sink, transcritical cycles can introduce small temperature differences during heat rejection, as shown in Fig. 1. This generally requires larger heat transfer surfaces when considering a fixed PPTD. Examining a fixed heat transfer surface for the heat exchanger is impractical due to the limited availability of heat transfer correlations in the literature that adequately model subcritical and supercritical heat exchangers [52]. Furthermore, the aim of this research is to examine the thermodynamic potential, rather than the financial potential. For the latter it should also be taken into account that transcritical cycles generally require smaller compressors [27]. However, it should be emphasized that in practical applications, a compromise may have to be made between the pinch point and the size of the heat exchanger. More information on the PPTD can be found in Section 2.2. For the IHX, where no phase change occurs, a fixed effectiveness of 0.75 is used. To facilitate a valid comparison between the cycle with and without the IHX, the IHX has been engineered to exhibit a relatively high heat exchange effectiveness. Nevertheless, the used effectiveness is still within the range of effectiveness's used in the literature [53–57]. Based on this effectiveness the refrigerant outlet states can be determined.

2.1.3. Expansion valve model

The expansion valve is assumed to be isenthalpic. The expansion losses in heat pumps employing conventional refrigerants are generally small [21]. For transcritical cycles however, the large pressure difference results in a higher potential of recovering the expansion work. Often studied expansion work recovery devices are expanders [58,59] and ejectors [60,61]. Whereas use of an expansion recovery device could be beneficial, it is not considered in this study, because it would be no fair comparison when not implementing financial and technical aspects. The potential of integrating an expander or ejector in transcritical cycles is however stressed.

2.1.4. Heat pump performance parameters

Once all heat pump cycle states are determined, the COP can be calculated. The COP is calculated based on the amount of process heat supplied ($\dot{Q}_{process}$) and the compressor power ($\dot{W}_{comp}$) as shown in Eq. (3):

$$COP = \frac{\dot{Q}_{process}}{\dot{W}_{comp}} \tag{3}$$

Next to the COP, the volumetric heating capacity (VHC) is a particularly important parameter as it gives an indication of the compressor size. For low VHCs, large compressors or high-speed compressors will be needed, driving up the heat pump investment cost. The VHC is calculated based on the volumetric efficiency, the density of the refrigerant at the compressor inlet ($\rho_{comp,in}$) and the difference in enthalpy over the condenser or gas cooler as shown in Eq. (4).

$$VHC = \eta_{vol} \cdot \rho_{comp,in} \cdot (h_{cond,in} - h_{cond,out}) \tag{4}$$

2.1.5. Model validation

To validate the thermodynamic model, case studies reported in the literature are simulated and the COP is compared. Next to implementing the heat source and sink boundary conditions, modeling assumptions such as PPTD or efficiencies are also adapted. An overview of the COP simulated by the thermodynamic model of this work and the COP reported in the literature can be found in Table 1. This table shows that the outcomes of the model align well with the results reported within the literature. Possible explanations for the small differences in COP could be differences in the REFPROP version, or rounding in the reported boundary conditions and results.

Table 1
Comparison of the developed model with the models reported in the literature.

Refrigerant	COP: Current work	COP: Literature	Deviation (%)	Reference
Propane	2.63	2.66	1.26	[62]
Ethanol	3.66	3.62	1.1	[63]
R161	4.14	4.04	2.47	[64]

2.2. Optimization model

In the optimization algorithm, the COP calculated by the thermodynamic model is maximized. To recap, the thermodynamic model requires 4 input variables: superheat at the evaporator (ΔT_{sh}), subcooling at the condenser (ΔT_{sc}), pressure during heat extraction (p_{low}) and pressure during heat delivery (p_{high}), in addition to the boundary conditions which stay fixed throughout the optimization. For each working fluid, both the heat pump cycle with and without IHX are optimized.

The objective function contains many local maxima, hence a state-of-the-art global optimizer implemented in SciPy [65] is used to find the global optimum. The basin-hopping global optimizer was chosen as it showed the most robust and best results for a specified number of function evaluations. Prior to running the basin-hopping algorithm, a dual annealing optimization with a low number of function evaluations is performed to provide an initial guess for the basin-hopping algorithm.

In the optimization method several constraints are implemented on the output values. These constraints cannot be directly applied by putting bounds on the input variables because they require an evaluation of the actual heat pump cycle using the thermodynamic model. Hence penalties (i.e. soft constraints) are applied to the objective function when the constraints are not met. The penalty functions are tuned so that the optimization algorithm quickly converges to a solution for which none of the constraints are violated. Soft constraints are applied on three output values, namely the PPTD at the condenser or gascooler, the PPTD at the evaporator and the presence of wet compression. Constraints are imposed on the PPTD, because the COP would be optimal for a zero PPTD, which would require infinitely large heat exchangers. Therefore, a PPTD of 5 K is imposed, which gives a suitable trade-off between COP and heat exchanger size [41]. Within each function evaluation of the optimization, the PPTD between working fluid and secondary medium is determined by using an separate optimizer to find the location at which the temperature difference between the two fluids is minimal.

The optimization strategy is computationally expensive due to the many local maxima of the objective function and the high number of working fluids considered. Hence, several techniques are applied to speed up the optimization. First, the optimization can be parallelized over all available processor cores, so that on each core the cycle is optimized for a different working fluid. Second, the bounds applied on the optimization variables are based on the working fluid's properties. By reducing the search space the optimization can be accelerated.

Overall, the optimization problem can be presented by:

$$\begin{aligned}
&Maximize && COP = f(p_{low}, p_{high}, \Delta T_{sh}, \Delta T_{sc}) \\
&Subject\ to && PPTD_{high} = f(p_{high}, \Delta T_{sc}) \geq 5 \\
& && PPTD_{low} = f(p_{low}, \Delta T_{sh}) \geq 5 \\
& && x_{comp,min} = f(p_{low}, p_{high}, \Delta T_{sh}) \notin [0, 1] \\
& && p_{low}^{L} \leq p_{low} \leq p_{low}^{U} \\
& && p_{high}^{L} \leq p_{high} \leq p_{high}^{U} \\
& && \Delta T_{sh}^{L} \leq \Delta T_{sh} \leq \Delta T_{sh}^{U} \\
& && \Delta T_{sc}^{L} \leq \Delta T_{sc} \leq \Delta T_{sc}^{U}
\end{aligned}$$

with $x_{comp,min}$ the minimum refrigerant quality that occurs during the compression process, and the superscript 'L' referring to lower boundary and 'U' to upper boundary.

2.3. Working fluid selection

Most studies are restricted to refrigerants that are currently used in practice. In this study however, all pure fluids within REFPROP 10.0 are being considered as potential working fluid. These working fluids are first screened in terms of environmental aspects, thermal stability, toxicity and flammability. Only if they pass the screening procedure they will be simulated. Additional elimination of working fluids may follow during post-processing when the enforced technical constrains, explained in Section 2.4, are not respected.

2.3.1. Environmental aspects

All working fluids that have a GWP below 150 and do not deplete the ozone layer are considered in this study. In this way, the EU-regulations regarding fluorinated GHG [66] and substances that deplete the ozone layer [67] are met.

2.3.2. Thermal stability

The thermal stability/reactivity of the working fluid at higher temperatures can be characterized by the instability grade of the NFPA 704 standard [68]. This grade rates the chemical stability of a substance at elevated pressures and temperatures on a scale from 0 to 4. Substances with an instability grade of 1 can already become unstable at elevated pressures and temperatures. Therefore, working fluids with an instability grade equal to, or higher than, 1 are disregarded. Examples of well performing working fluids that are discarded due to their low chemical stability are: dimethyl ether, dimethyl carbonate, 1-pentene, 1,3-butadiene, trans-2-butene, or 1-butyne.

Whereas the NFPA 704 thermal stability grade gives an indication of violent chemical changes at higher pressures and temperatures such as explosive decomposition or detonation, the refrigerant can also decompose over time when subjected to high pressures and temperatures (i.e. thermolysis). Decomposition of the working fluid can lead to a reduction in thermal efficiency because of the change in operating conditions [69]. Moreover, decomposition products such as non-condensable gases or deposits could damage the components and induce safety concerns [69]. In addition, if the working fluid would depreciate over a short time interval it would show less favorable financial appraisal than expected [70]. Therefore, it is crucial that the working fluid shows no, to low, thermolysis at the targeted temperatures and pressures. Consequently, working fluids that start to decompose below 200 °C are eliminated.

2.3.3. Flammability

Flammability and explosion concerns may withhold use of refrigerants such as hydrocarbons. An exception is the chemical industry where the processes may already be protected [71]. However, when correctly handled and installed, flammable refrigerants are safe to use [72]. Several use cases of such flammable refrigerants at high temperatures and pressures can be found. Bamigbetan et al. [73] constructed a laboratory-scale HTHP, supplying heat up to 115 °C. The heat pump is a cascaded cycle making use of propane as low-temperature cycle and propane as high-temperature cycle, based on components that are commercially available. Furthermore, several HTHP manufacturers (Mayekawa, Johnson Controls, etc.) offer commercial available HTHPs making use of hydrocarbons for supply temperatures up to 145 °C [74]. In the field of ORCs, the use of hydrocarbons is more prevalent. Galindo et al. [75], constructed an experimental ORC making use of ethanol as working fluid to recover waste heat from a gasoline engine. For this set-up exhaust gas inlet temperatures up to 673 °C were tested. Furthermore, several ORC manufacturers (Ormat, Turboden, Atlas Copco, etc.) make use of hydrocarbons such as cyclo-pentane, iso-pentane or n-butane for waste heat temperatures well above 200 °C [76]. Therefore, no constraint is placed upon the flammability. Instead, in contrast to most literature, two scenarios are considered: one where flammable fluids are allowed and one where they are not allowed. For the flammability grade the ASHRAE 34 standard [77] is used which classifies the flammability in four grades. In the scenario that flammability is a concern, highly flammable fluids (class 3) and flammable fluids (class 2) will be disregarded whereas non-flammable fluids (class 1) and mildly flammable fluids (class 2L) will be considered.

Whereas no direct limitation is placed upon the flammability grade a limitation will be placed upon the auto-ignition temperature. If the compressor discharge temperature without (external) cooling method exceeds the auto-ignition temperature the fluid will be eliminated from the results. In this way the system can safely operate even when the (external) cooling fails.

2.3.4. Toxicity

Ideally, the refrigerant is non-toxic. However, toxic refrigerants such as ammonia are widely used in heat pumps and refrigeration machines. Ammonia has the highest toxicity grade according to the ASHRAE 34 standard (class B) and a health-grade of 3 out of 4 according to the NFPA 704 standard. With ammonia set as boundary for the maximum toxicity, working fluids with an NFPA 704 health-grade of 4 will be disregarded from the analysis.

An overview of the working fluid selection can be found in Appendix. In this appendix it is indicated whether the working fluid passed the imposed GWP limitation, ozone depletion potential (ODP) limitation, NFPA 704 instability limitation and NFPA 704 health limitation. For some working fluids no NFPA 704 standard was found, so the instability and health grade was named ‘unknown’. These working fluids were not eliminated by the screening procedure. However, when these working fluids show to be amongst the best performing working fluids, its instability grade and health hazard will be carefully studied.

2.4. Technical constraints

As indicated in the optimization model and fluid selection, some working fluids may not be considered because they result in unrealistic technical requirements. The imposed technical requirements are described in the upcoming sections.

2.4.1. Compressor discharge temperature

The compressor discharge temperature should be kept as low as possible for various reasons. First of all, the refrigerant-oil mixture might become thermally unstable at higher temperatures when the compressor is lubricated [4]. In addition, oil degradation may occur when subjected to prolonged high temperatures [73]. Furthermore, a high compressor discharge temperature poses challenges in the heat management and wear of the compressor and materials of the equipment [4].

Whereas high compressor discharge temperatures may cause severe issues when not appropriately handled, no constraint is placed upon the compressor discharge temperature because several techniques exist to reduce it. Examples are: two-phase compression, vapor or liquid injection and intercooling [78,79]. These cooling techniques can reduce the specific compressor power. However, this involves a trade-off because less heat will be delivered during heat rejection when the discharge temperature decreases. Furthermore, for applications with a large temperature glide, the reduction of the compressor discharge temperature leads to an increase in pressure during heat rejection in order to respect the implemented PPTD, as can be observed in Fig. 4. A similar behavior was observed in the work of Arpagaus et al. [33], who found that for applications with large temperature glide a transcritical cycle with parallel compression did not lead to improved COPs compared to a conventional transcritical cycle with IHX. The reason for this is that the cycle making use of parallel compression reduces the discharge temperature.

For these reasons, it was found that these methods of reducing the discharge temperature did not offer any advantages in terms of

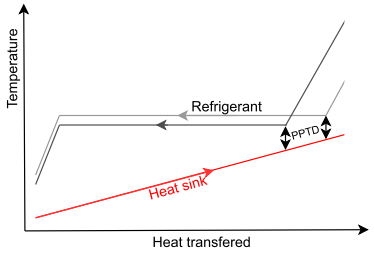

Fig. 4. Illustration of the effect of a decrease of compressor discharge temperature on the heat rejection pressure.

COP. However, no cycle configurations are implemented to reduce the compressor discharge temperature because multiple configurations exists. Furthermore, no exact boundary can be defined on the maximum discharge temperature as this strongly depends on the compressor design.

2.4.2. Pressure ratio

The pressure ratio should be as low as possible. For high pressure ratios, multiple compression stages may be required. This would strongly drive up the investment cost and the complexity of the heat pump system. With single compressor units typically having a pressure ratio about 4–5 [80–83], this study considers a maximum pressure ratio of 20 so that no more than two compression stage should be used.

2.4.3. Pressure levels

The maximum allowable discharge pressure for most commercial refrigerant compressors is around 30 bar [4,80–82,84,85]. However, some compressors are being designed for pressures in the range of 50–60 bar [4,5,80,81,84], e.g for use of ammonia or R32. Furthermore, some transcritical CO2 compressors are specifically designed for discharge pressures up to 140–150 bar [5,27,80,81]. Because of, amongst others, the low pressure ratio of CO2 compressors, these compressors are not suitable for other refrigerants [27]. Therefore, a maximum compressor discharge pressure of 60 bar is assumed in this study.

Next to the limitations on maximum discharge pressure, there is a limitation on the minimum pressure within the heat pump system. If the minimum pressure is below the atmospheric pressure, air may infiltrate in the system, if not well sealed. This may introduce undesired effects on the operation of the heat pump system. Furthermore, when the refrigerant is flammable, flammability issues may occur when air infiltrates. Therefore, in this work, the minimum pressure should be above 1 bar for flammable or highly flammable fluids and above 0.5 bar for non-flammable or mildly flammable fluids. This constraint caused for example the elimination of dimethyl carbonate.

2.5. Boundary conditions

As previously stressed, transcritical operation can show beneficial effects in the event of large temperature glides at the heat sink side. Therefore, three representative industrial case studies with large heat sink temperature glides are selected, rather than generic data. The temperature glides at the heat sink side are 60 K, 81 K and 105 K.

2.5.1. Case I: Thermal oil heating

The energy-intensive industry often employs indirect heat exchanger networks (HEN) using intermediate fluids such as steam or thermal oil to provide heat. Direct integration could involve topological disadvantages, limited operational flexibility and controllability of the overall plant and chemical and safety hazards [86]. HEN covers these disadvantages, but at reduced energy conservation opportunities because of the exergy destruction impaired in employing an intermediate heat carrier.

This case study considers the thermal oil heating from a HEN. The data was collected and aggregated from bilateral meetings with industry. At the industrial site, thermal oil (Therminol 66) is heated from 140 °C to 200 °C, corresponding with a temperature glide of 60 K. The heat is currently delivered by use of a natural gas boiler. However, as the same integrated site has a pressurized hot water waste heat stream available at 100 °C, the natural gas boiler could be replaced by a heat pump valorizing this waste heat stream. The temperature levels, mass flow rate and pressure level of the heat source and sink are reported in Table 2.

2.5.2. Case II: Superheated steam drying

Superheated steam drying (SSD) is a well-known drying technology which recently has gained importance and became a viable technology [87]. In the SSD process, the superheated steam acts as a heat source and drying medium to remove water from the product [88]. This is often a closed-loop process where the majority of the steam is recirculated to be superheated. The excess steam of the process, obtained by the water evaporation, can be used as a latent heat source for superheating the process steam.

The data reported in the work of Bang-Møller et al. [89] is used for the case study. In their work a superheated steam dryer is used for drying of wet wood (42% water), which is used for a combined heat and power plant. In this work the superheated steam drying process is isolated and heat pump integration is considered. A schematic of the heat pump assisted superheated steam drying process can be found in Fig. 5. In this particular process, superheated steam needs to be heated from 116 °C to 197 °C. For this, some superheated steam, with a condensation temperature of 100 °C, is available at 115 °C. If the slightly superheated excess steam completely condenses, about 298 kW_{th} of heat can be extracted. Considering the addition of compression work in the energy balance this should be sufficient to deliver the 370 kW_{th} of heat which is demanded for superheating the process steam.

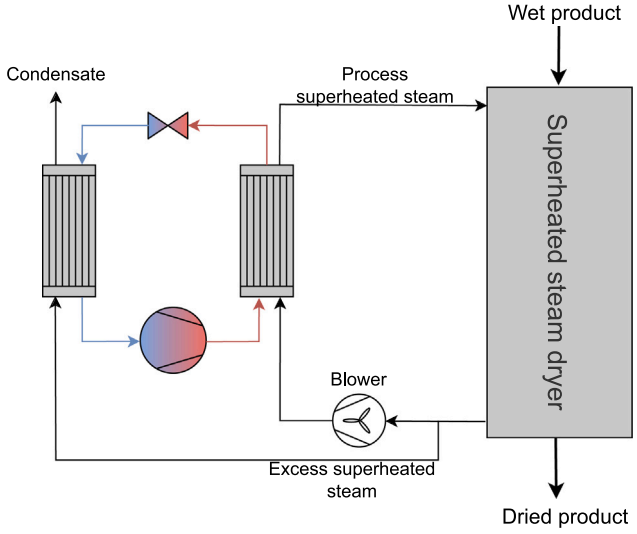

Fig. 5. Heat pump assisted superheated steam dryer configuration.

The temperature levels, mass flow rate and pressure level of the heat source and sink can be found in Table 3.

2.5.3. Case III: Spray drying with external heat source

Wang et al. [32] investigated heat recovery for spray dryers in the food industry. According to their study the ambient inlet air of spray dryers is typically heated to about 200 °C or higher. The exhaust air is typically in the temperature range of 60–80 °C, with dew points around 35–40 °C. Their simulations, which indicated that transcritical cycles have the best performance, showed that about 40% of the air

Table 2
Information on heat source and heat sink for the thermal oil heating case study.

	Heat source				Heat sink			
Fluid	p [bar]	$\dot{m}$ [kg/s]	T_{in} [°C]	Fluid	p [bar]	$\dot{m}$ [kg/s]	T_{in} [°C]	T_{out} [°C]
Water	20	20	100	Therminol 66	1	10	140	200

Table 3
Information on the heat source and heat sink for the SSD case study, data according to [89].

	Heat source				Heat sink			
Fluid	p [bar]	$\dot{m}$ [kg/s]	T_{in} [°C]	Fluid	p [bar]	$\dot{m}$ [kg/s]	T_{in} [°C]	T_{out} [°C]
Superheated steam	1	0.13	115	Superheated steam	1	2.27	116	197

Table 4
Information on the heat source and heat sink for the spray drying case study with an external waste heat source.

	Heat source				Heat sink			
Fluid	p [bar]	$\dot{m}$ [kg/s]	T_{in} [°C]	Fluid	p [bar]	$\dot{m}$ [kg/s]	T_{in} [°C]	T_{out} [°C]
Water	1.5	1.69	100	Dry air	1	1	95	200

heating load could be provided by use of heat pumps, lowering the energy costs with more than 20%. Providing the complete air heating load (i.e. heating the air up to 200 °C) with use of the exhaust air is not possible because this would require unfeasible large temperature lifts. A potential solution is utilizing an external waste heat source with a suitable temperature level and energy content, so that the inlet air can be directly heated up to 200 °C without the use of an auxiliary heating system.

In this generic case study, an external waste heat stream at a temperature level of 105 °C will be considered. Nevertheless, the exhaust air of the spray dryer will still be used for preheating the dry inlet air as shown in Fig. 6. It is assumed that the dry inlet air has a mass flow rate of 1 kg/s and is heated up to 60 °C by the exhaust air. The preheated dry inlet air is then further preheated up to 95 °C by use of the hot water waste heat, considering a PPTD of 10 K in the respective counter flow heat exchanger. If the outlet temperature of the hot water stream is assumed to be 100 °C, it would imply that there is 1.69 kg/s of hot water available at 100 °C to heat the preheated inlet air from 95 °C to 200 °C by use of a heat pump. This implies a slightly crossing temperature profile of the heat source and sink.

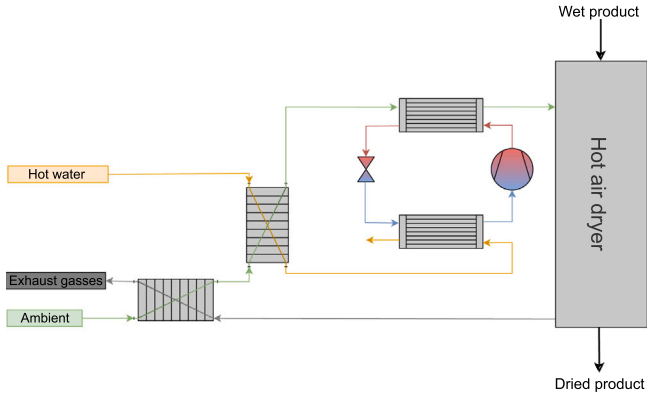

Fig. 6. Considered heat recovery configuration for spray drying case study.

An overview of the process parameters of the heat pump system can be found in Table 4.

3. Results and discussion

For each case study the best performing working fluids with their optimized operating conditions (p_{low}, p_{high}, ΔT_{sh} and ΔT_{sc}) are reported in a table. The table also reports the pressure ratio (PR), COP, VHC, compressor discharge temperature ($T_{c,d}$), cycle type, i.e. subcritical (SC) or transcritical (TC), and whether or not the cycle optimally makes use of an IHX.

3.1. Case I: Thermal oil heating

The results of the best performing working fluids in terms of COP for the thermal oil heating case can be found in Table 5.

3.1.1. Working fluids and performance

Based on the reported results in Table 5 it can be observed that classical subcritical cycles have a slightly higher COP compared to transcritical cycles for the case study with a heat sink temperature glide of 60 K. For subcritical cycles COPs up to 3.34 are observed, while for transcritical cycles COPs up to 3.30 are observed. Acetone, benzene and ethanol, which are not yet introduced for use in HTHPs, are found to be the best performing fluids for subcritical cycles whereas cyclobutene, R1336mzz(Z) and R1233zd(E) are found to be the best performing fluids inducing transcritical cycles. All reported fluids, with the exception of methanol, have a higher COP when an IHX is added. Methanol already has a compressor discharge temperature of about 300 °C, even without IHX. Addition of an IHX would strongly increase this temperature and would therefore also induce a lot of exergy destruction.

3.1.2. Operating conditions

Both the subcritical and transcritical cycles have a considerable amount of subcooling (i.e. ΔT_{sc}) in order to maximize the heat output for a given amount of compression work. These high subcooling values can be observed in the T,s-diagrams of the best performing subcritical and transcritical cycles as illustrated in Fig. 7. In these cycles an IHX is used. Typically the optimal amount of subcooling is adapted such that, next to an already existing pinch point, a new pinch point almost appears at the location where the refrigerant leaves the heat exchanger. This behavior is also observed in other literature [39]. A similar behavior is observed for the superheat. This figure also shows that the strong superheat at the condenser inlet for subcritical cycles leads to a high compressor discharge temperature. For transcritical cycles however, the discharge temperature is limited because of the temperature match at the gas cooler.

Next to the lower compressor discharge temperature it can be observed that transcritical cycles have much higher VHCs and considerably lower pressure ratios. For the reported transcritical cycles the

Table 5
Results of the best performing fluids for the thermal oil heating case.

Fluid	p_{low} [bar]	p_{high} [bar]	PR [–]	ΔT_{sh} [°C]	ΔT_{sc} [°C]	COP [–]	VHC [kJ/m^3]	$T_{c,d}$ [°C]	Cycle [–]	IHX [–]
Acetone	2.5	23.1	9.4	0.0	44.2	3.34	2545	250	SC	Yes
Benzene	1.2	13.6	11.7	0.0	51.5	3.33	1315	232	SC	Yes
Ethanol	1.3	23.4	18.2	10.2	43.0	3.31	1858	300	SC	Yes
Cyclobutene	10.6	53.3	5.0	10.4	29.9	3.30	7454	231	TC	Yes
Methanol	2.1	31.7	14.9	0.7	42.6	3.29	3047	296	SC	No
Cyclohexane	1.1	13.7	12.1	9.7	56.3	3.29	1243	213	SC	Yes
Cyclopentane	2.8	25.0	8.8	10.4	50.7	3.29	2681	224	SC	Yes
Pentane	4.1	31.2	7.5	10.3	46.6	3.28	3371	210	SC	Yes
R1336mzz(Z)	4.9	35.9	7.4	10.3	26.4	3.26	3815	209	TC	Yes
R1233zd(E)	7.4	43.1	5.9	10.0	21.5	3.26	5338	217	TC	Yes
Isopentane	5.1	35.0	6.9	10.1	42.2	3.26	3878	208	TC	Yes
Isohexane	2.1	21.8	10.5	9.6	57.1	3.25	1945	207	SC	Yes
3-Methylpentane	1.9	20.7	10.9	10.3	58.5	3.24	1812	206	SC	Yes
2.3-Dimethylbutane	2.2	22.5	10.3	9.0	59.4	3.23	2019	205	SC	Yes
2.2-Dimethylbutane	2.7	25.7	9.4	9.4	58.4	3.22	2357	205	SC	Yes

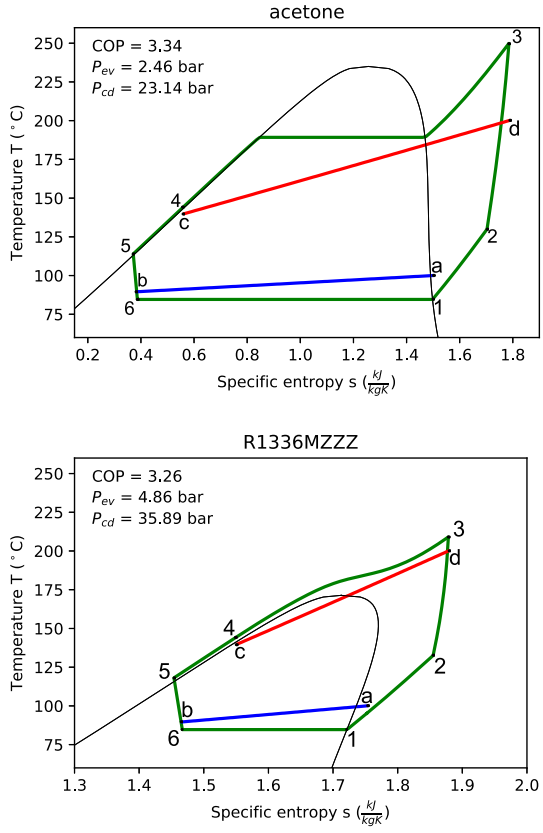

Fig. 7. T,s-diagram, with scaled entropy for secondary fluid, for the best performing subcritical cycle (top) and transcritical cycle (bottom) for the thermal oil heating case study.

VHC varies between 3815–7454 kJ/m^3 and the pressure ratio between 5–7.5, whereas for subcritical cycles the VHC varies between 1065–3371 kJ/m^3 and the pressure ratio varies between 7.5–18.2. Therefore, use of transcritical cycles could already be beneficial for heat sink temperature glides of 60 K and lower. Cyclobutene, whose potential is not yet reported in literature, is found to be particularly suitable for this because of the combination of it high COP and high VHC. A particular disadvantage of transcritical operation however is the associated high compressor discharge pressure, which requires high-pressure compressor series. For the subcritical cycles the compressor discharge pressure varies between 13.6–31.7 bar whereas for the transcritical cycles it varies between 35–53.3 bar.

3.2. Case II: Superheated steam drying

The results of the working fluids with the highest COP for the SSD case are reported in Table 6.

3.2.1. Working fluids and performance

Now, with a temperature glide of 81 K at the heat sink side, transcritical cycles show better performance in terms of COP compared to subcritical cycles. The COP of the best performing transcritical cycle is 4.32 whereas the COP of the best performing subcritical cycle is 4.13. Consequently, a COP increase of 4.6% can be achieved by using transcritical cycles. The HFOs or Hydrochlorofluro-olefins (HCFOs) R1336mzz(Z), R1234ze(Z) and R1233zd(E) are found to be the best performing fluids for transcritical cycles. These working fluids are already being experimentally investigated for HTHPs, but at lower temperatures (<160 °C), operating in the subcritical regime [42,90,91]. Its potential for higher operational temperatures by operating in the transcritical region is yet to be unlocked. Ethanol, methanol and acetone are found to be the best performing fluids for subcritical cycles. Again, the most optimal heat pump cycle always makes use of an IHX, with the exception of methanol.

3.2.2. Operating conditions

As for the thermal oil heating case study, the subcooling is high and almost induces a new pinch point. The amount of superheat however, is now often close to zero because of the latent heat source. The transcritical cycles again show much higher VHCs, lower pressure ratios and lower compressor discharge temperatures on average. For almost all transcritical cycles, with the exception of cyclobutene and cis-2-butene, the minimum possible compressor discharge temperature of 202 °C is observed. The compressor discharge pressures for transcritical cycles are again high and are somewhat increased compared to the thermal oil heating case, even though the heat sink outlet temperature of the SSD case study (197 °C) is 3 °C lower compared to the thermal oil heating case study (200 °C). The increase in compressor discharge pressure is a result of the lower heat sink inlet temperature, while the heat source temperature remains similar for similar heat source temperatures as can be observed from Fig. 8, where the isobars are drawn. For lower heat sink inlet temperature the potential for the IHX decreases. Consequently, higher compressor discharge pressures are observed. This causes for example an increase of compressor discharge pressure of 26% for R1336mzz(Z) when comparing the SSD case with the thermal oil heating case.

Table 6
Results of the best performing fluids for the superheated steam drying case.

Fluid	p_{low} [bar]	p_{high} [bar]	PR [–]	ΔT_{sh} [°C]	ΔT_{sc} [°C]	COP [–]	VHC [kJ/m^3]	$T_{c,d}$ [°C]	Cycle [–]	IHX [–]
R1336mzz(Z)	6.2	43.3	6.9	0.0	50.4	4.32	5607	202	TC	Yes
R1234ze(Z)	12.1	57.1	4.7	1.5	29.1	4.31	9488	202	TC	Yes
R1233zd(E)	9.3	47.8	5.1	1.1	45.5	4.30	7708	202	TC	Yes
Cyclobutene	13.1	54.3	4.1	2.3	53.9	4.29	10204	208	TC	Yes
Cis-2-Butene	12.8	55.6	4.4	1.5	41.6	4.26	9643	203	TC	Yes
Isopentane	6.4	40.0	6.2	0.0	66.2	4.26	5456	202	TC	Yes
Pentane	5.3	35.0	6.6	0	75.6	4.20	4746	202	TC	Yes
R1224yd(Z)	10.3	55.3	5.4	1.8	34.5	4.20	8256	202	TC	Yes
Acetone	3.3	23.1	7.1	2.99	68.0	4.20	3585	222	SC	Yes
Ethanol	1.9	22.4	12.0	0.0	64.9	4.13	2817	258	SC	Yes
Methanol	3.0	28.5	9.5	0.0	61.3	4.12	4307	267	SC	No
Cyclopentane	3.7	26.8	7.3	0.0	79.8	4.03	3732	204	SC	Yes
Benzene	1.6	14.2	9.1	0.0	78.2	4.01	1871	209	SC	Yes

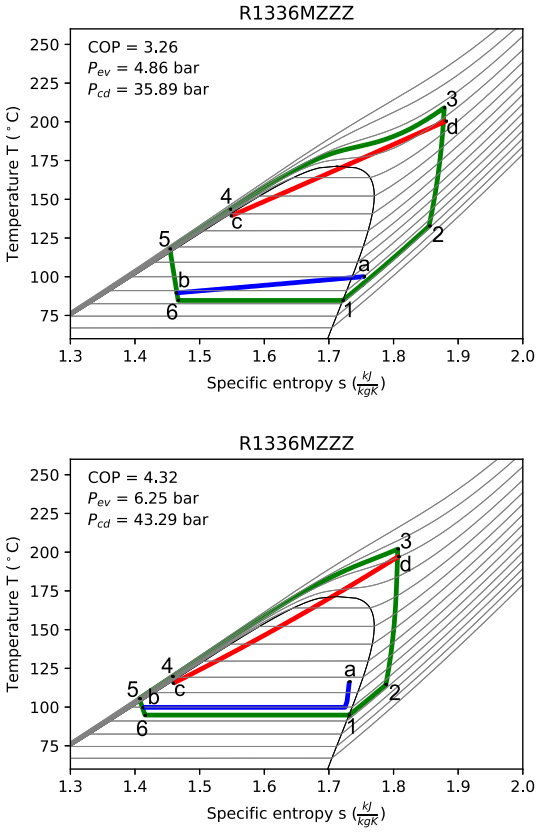

Fig. 8. T,s-diagram of R1336Mzz(Z), with scaled entropy for the secondary fluid and isobars, when applied to the thermal oil heating case study (top) and the SSD case study (bottom).

3.3. Case III: Spray drying with external heat source

The results of the best performing working fluids for the spray drying with external heat source case study are reported in Table 7.

3.3.1. Working fluids and performance

Now that the heat sink has a temperature glide of 105 K, transcritical cycles have even better performance compared to subcritical cycles. The best performing transcritical cycle with R1336mzz(Z) as working fluid has a COP of 4.25 while acetone as best performing subcritical cycle has a COP of 3.96. This corresponds to a COP increase of 7.3%. Acetone, methanol and ethanol are again the best performing subcritical fluids while R1336mzz(Z), R1233zd(E) and isopentane are the best performing transcritical fluids. R1234ze(Z) also showed good performance but was eliminated from the results because the imposed maximum compressor discharge pressure was exceeded due to the low potential for internal heat exchange.

3.3.2. Operating conditions

Similar operating conditions as for the previous case studies are found. Namely that transcritical cycles mostly have more favorable pressure ratios, VHCs and lower compressor discharge temperatures. However, again they have high compressor discharge pressures. Moreover, a similar behavior in optimal superheating and subcooling is observed as for previous cases.

3.4. Influence of the internal heat exchanger

Although the use of an IHX is common practice in heat pumps, its influence on the cycle performance for applications with high temperatures and large temperature glides at the heat sink is less studied. Therefore, this section analyzes the effect of the IHX on the cycle performance for the three considered case studies. Based on the results of the three case studies it can be observed that most working fluids can attain a higher COP when an IHX is included in the cycle. In order to examine the influence of an IHX on the cycle performance and operating conditions, the COP, pressure during heat delivery, pressure ratio and compressor discharge temperature for two subcritical fluids and two transcritical fluids are reported in Table 8, both for the scenario with IHX and without IHX. Acetone and benzene are selected as subcritical fluids whereas R1336mzz(Z) and R1233zd(E) are selected as transcritical fluids.

For the thermal oil heating case, it can be observed that the use of an IHX has a large influence on the heat pump cycle. For R1336mzz(Z) a COP increase of 22% and a gas cooler pressure decrease of 57% is observed, while the compressor discharge temperature increased with about 4 °C. For the other working fluids, smaller but still considerable COP increases and pressure decreases are being observed. Because of the decrease in pressure during heat release, the pressure ratio also decreased. For subcritical cycles however the increase in performance due to the use of an IHX is typically lower. R1336mzz(Z) showed an exceptionally strong increase in COP because of its overhanging fluid saturation curve. More generally, IHXs provide a very efficient way to avoid wet compression when wet fluids are used. The advantages of the IHX may come at the cost of an increased compressor discharge temperature. Especially for subcritical cycles, the compressor discharge temperatures show an increase when making use of an IHX. For transcritical cycles this is less of an issue.

For the SSD case similar conclusions as for the thermal oil heating case can be drawn. A difference however, is that now the minimum compressor discharge temperature is being achieved for the transcritical cycles regardless of the use of an IHX.

For the spray drying with external heat source, use of an IHX has minimal influence on the heat pump cycle states and therefore the COP

Table 7
Results of the best performing optimized fluids for the spray drying case study with external heat source.

Fluid	p_{low} [bar]	p_{high} [bar]	PR [–]	ΔT_{sh} [°C]	ΔT_{sc} [°C]	COP [–]	VHC [kJ/m^3]	$T_{c,d}$ [°C]	Cycle [–]	IHX [–]
R1336mzz(Z)	4.7	53.4	11.3	0.0	71.4	4.25	4855	205	TC	Yes
R1233zd(E)	7.2	52.9	7.4	11.4	66.5	4.18	6887	205	TC	Yes
Isopentane	5.0	43.1	8.6	11.4	83.4	4.14	4727	205	TC	Yes
Cyclobutene	10.4	56.0	5.4	11.4	74.9	4.12	9194	208	TC	Yes
Pentane	4.0	36.9	9.1	11.3	90.0	4.03	4009	205	TC	Yes
Acetone	2.4	23.6	9.8	11.3	90.3	3.96	2957	222	SC	Yes
Methanol	2.1	25.4	12.3	8.1	76.8	3.89	3233	296	SC	No
Ethanol	1.2	23.2	18.6	0.0	87.6	3.89	2141	250	SC	No
Cyclopentane	2.8	28.7	10.3	11.1	103.5	3.83	3156	205	SC	Yes
Benzene	1.1	15.5	13.6	10.8	104.7	3.77	1528	205	SC	No

Table 8
Influence of IHX on two subcritical fluids and two transcritical fluids for the three selected case studies.

Working fluid	IHX	COP [–]	p_{high} [bar]	PR [–]	$T_{c,d}$ [°C]
Case 1: Thermal oil heating					
R1336mzz(Z)	✓	3.26	35.9	7.4	209.1
	✗	2.67	56.2	11.3	205.0
R1233zd(E)	✓	3.26	43.1	5.9	217.3
	✗	2.80	55.8	7.5	205.0
Acetone	✓	3.34	23.1	9.4	249.9
	✗	3.18	25.9	10.2	222.6
Benzene	✓	3.33	13.8	11.7	232.5
	✗	3.11	15.6	13.3	205.0
Case 2: Superheated steam drying					
R1336mzz(Z)	✓	4.32	43.3	6.9	202.0
	✗	3.71	51.0	10.0	202.0
R1233zd(E)	✓	4.30	47.8	5.1	202.0
	✗	4.04	58.1	6.3	202.0
Acetone	✓	4.17	23.1	7.1	222.1
	✗	4.05	25.4	7.8	209.5
Benzene	✓	4.00	14.2	9.1	208.6
	✗	3.69	14.9	11.3	202.0
Case 3: Spray drying with external heat source					
R1336mzz(Z)	✓	4.25	53.4	11.3	205.0
	✗	4.24	54.4	11.6	205.0
R1233zd(E)	✓	4.18	52.9	7.4	205.0
	✗	4.11	59.8	8.3	205.0
Acetone	✓	3.96	23.6	9.8	221.5
	✗	3.94	24.1	10.0	218.9
Benzene	✓	3.77	15.4	10.6	205.5
	✗	3.77	15.5	13.6	205.5

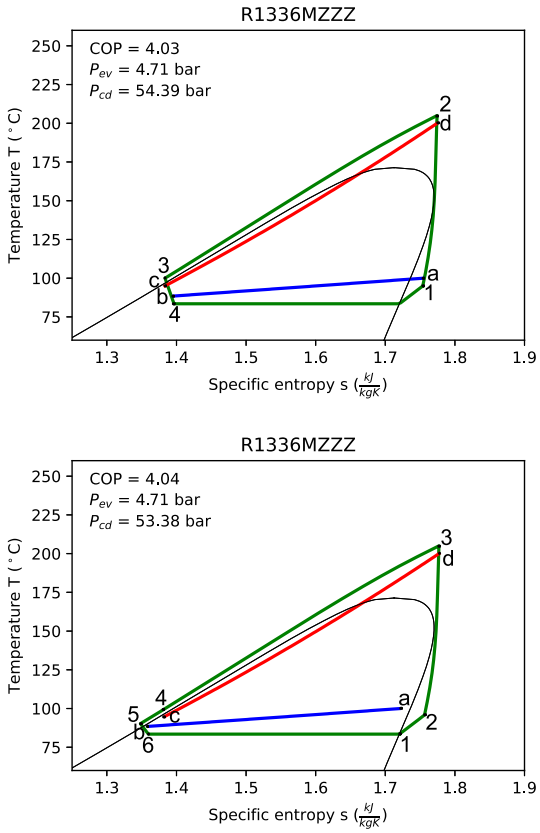

Fig. 9. T,s-diagram of R1336mzz(Z), with scaled entropy for secondary fluid, without (top) and with (bottom) IHX for the spray drying with external heat source case study.

and operating conditions. The reason is that the heat sink and heat source inlet temperatures slightly cross. Consequently, only a limited amount of heat can be internally transferred as displayed in Fig. 9.

3.5. Influence of flammability

All reported subcritical fluids (e.g. acetone, benzene or methanol) are highly flammable. For the transcritical cycles, some highly flammable fluids are observed as well (e.g. isopentane, cyclobutene). However, HFOs and HCFOs were often the best performing fluids with transcritical cycles. The HFOs/HCFOs are either inflammable or mildly flammable. Therefore, if highly flammable fluids or flammable fluids would not be allowed on the industrial site, the impact for the transcritical cycles would be minimal, or there would be no impact at all. For the subcritical cycles however the impact would be larger. The only appropriate working fluid would be water. Using water as working fluid for these selected cases shows however lower COPs and less favorable operating conditions compared to the HFOs/HCFOs. The results for water as working fluid for each case study can be found in Table 9.

This table shows that use of water as a refrigerant is at first sight less advantageous compared to the HFOs/HCFOs. Firstly, the pressure during heat extraction is below the atmospheric pressure. In addition to potential air infiltration this also induces a low density at the compressor's inlet and therefore a low VHC ranging from 1065–1477 kJ/m^3. The VHCs of the HFOs/HCFOs on the other hand range from 3815–9488 kJ/m^3. Moreover, the low pressures during heat extraction result in large pressure ratios. Pressure ratios in the range of 12.89–21.20 are observed, whereas for the HFOs/HCFOs they range from 4.7 to 11.7. Furthermore, the compressor discharge temperature is high (up to 569 °C) when using water as refrigerant. Therefore a large cooling system will be required, whereas for the HFOs/HCFOs the compressor discharge temperatures are low and no cooling system is needed. Compared to the best performing HFO/HCFO, the COP is 5.5%, 15.2% and 22.5% lower for the oil heating case, SSD case and the hot

Table 9
Results of the best performing non-flammable or mildly flammable subcritical cycles for the selected case studies.

Case	Fluid	p_{low} [bar]	p_{high} [bar]	PR [–]	ΔT_{sh} [°C]	ΔT_{sc} [°C]	COP [–]	VHC [kJ/m^3]	$T_{c,d}$ [°C]	IHX [–]
Oil heating	Water	0.58	12.2	21.2	0.0	43.9	3.09	1065	569	No
SSD	Water	0.84	10.8	12.9	0.0	62.4	3.75	1477	488	No
Hot air drying	Water	0.54	9.8	18.1	0.0	79.1	3.47	1045	534	No

air drying case respectively. Again, it can be observed that for larger temperature glides, transcritical cycles become more efficient.

4. Conclusion

A unique thermodynamic model is developed, allowing for robust optimization, and is applied to three relevant case studies, namely: thermal oil heating, spray drying and superheated steam drying. These case studies have heat sink temperature glides of respectively 60 K, 81 K and 105 K.

The optimized results show that starting from a heat sink temperature glide of 60 K, transcritical cycles allow for higher COPs. For the case study with a heat sink temperature glide of 81 K, transcritical cycles allowed for a COP increase of 4.6% whereas this increased to 7.3% for the case with a heat sink temperature glide of 105 K. Transcritical cycles also introduce higher volumetric heating capacities, require lower pressure ratios and have lower compressor discharge temperatures. Furthermore, for high heat sink temperature glides, cooling techniques to reduce the compressor discharge temperature increase the condenser/gas cooler pressure and decrease the COP. Therefore, from a practical and financial point of view transcritical cycles may be recommended for heat sink temperature glides below 60 K.

The best performing transcritical working fluids are HFOs and HCFOs. More specifically R1336mzz(Z), R1234ze(Z) and R1233zd(E) often showed the best performance. However, the natural refrigerants cyclubutene, cis-2-butene, isopentane and pentane in the transcritical regime also shows similar thermodynamic advantages over subcritical cycles. These working fluids, with the exception of cyclobutene and cis-2-butene, are well-known but are not yet used in the transcritical regime. For the subcritical cycles, acetone, ethanol and methanol were marked as best performing working fluids. These working fluids are not yet introduced for use in high-temperature heat pumps. They are however highly flammable. If these flammable working fluids would be neglected, water shows the highest COP as subcritical working fluid. Unfortunately, water results in strongly reduced COPs and volumetric heating capacities and strongly increased pressures ratios and compressor discharge temperatures, hence far less favorable financial appraisal is expected.

The results also shows that optimization of the superheat, and in particular subcooling, have a large influence on the COP. The degree of subcooling and superheating should be controlled so that, next to an already existing pinch point, a new pinch point is almost created at the location where the refrigerant leaves the heat exchanger. Moreover, for transcritical cycles, the gas cooler pressure is also of particular importance.

Furthermore, the influence of an internal heat exchanger was studied in this work. Internal heat exchangers often allow for a large increase in COP and a decrease in compressor discharge pressure and therefore pressure ratio. The influence was especially high for the transcritical cycles. However, for some scenarios, especially in case of subcritical cycles, the compressor discharge temperature increased, although this was not necessarily the case for transcritical cycles. The potential of the internal heat exchanger however diminishes as the heat source inlet temperature and heat sink outlet temperature becomes smaller.

One overall disadvantage of the transcritical cycles is the high compressor discharge pressure. If compressor technologies can be developed able to handle these high pressures transcritical cycles are superior compared to subcritical cycles starting from heat sink temperature glides of 60 K or even lower.

Nomenclature

GHG	Greenhouse gas
GWP	Global warming potential
h	Enthalphy (kJ/kg)
HC	Hydrocarbon
HCFO	Hydrochlorofluro-olefin
HEN	Heat exchanger network
HFO	Hydrofluro-Olefins
IHX	Internal heat exchanger
$\dot{m}$	Mass flow rate (kg/s)
NFPA	National Fire Protection Agency
ODP	Ozone depletion potential
ORC	Organic Rankine cycle
p	Pressure (Pa)
PR	Pressure ratio
PPTD	Pinch point temperature difference (K)
$\dot{Q}$	heat transfer rate (W)
SSD	Superheated steam drying
SC	Supercritical
T	Temperature (°C)
TC	Transcritical
VHC	Volumetric heating capacity (kJ/m^3)
$\dot{W}$	Power (W)

CRediT authorship contribution statement

Elias Vieren: Conceptualization, Investigation, Methodology, Software, Writing – original draft, Writing – review & editing. **Toon Demeester:** Writing – review & editing. **Wim Beyne:** Writing – review & editing. **Alessia Arteconi:** Writing – review & editing. **Michel De Paepe:** Writing – review & editing. **Steven Lecompte:** Writing – review & editing, Project administration, Funding acquisition, Supervision.

Declaration of competing interest

The authors declare the following financial interests/personal relationships which may be considered as potential competing interests: Steven Lecompte reports financial support was provided by Flemish Government and Flanders Innovation Entrepreneur ship (VLAIO).

Data availability

No data was used for the research described in the article.

Acknowledgments

We gratefully acknowledge the financial support of the Flemish Government and Flanders Innovation & Entrepreneurship (VLAIO), Belgium through the Moonshot project Upheat-INES (HBC.2020.2616).

Appendix

See Table A.1.

Table A.1
Working fluid screening.

Short name	Short formula	Critical temperature (°C)	Critical pressure (bar)	Passed working fluid screening?	GWP ≤ 150?	ODP ≈ 0?	NFPA health hazard ≤ 4?	NFPA Reactivity = 0?
1,3-Butadiene	C4H6	152.0	43.1	No	Yes	Yes	Yes	No
1-Butyne	C4H6	158.9	41.4	No	Yes	Yes	Yes	No
1-Pentene	C5H10	192.6	36.0	No	Yes	Yes	Yes	No
2,2-Dimethylbutane	C6H14	216.9	31.4	Yes	Yes	Yes	Yes	Yes
2,3-Dimethylbutane	C6H14	227.5	31.6	Yes	Yes	Yes	Yes	Yes
3-Methylpentane	C6H14	232.9	31.8	Yes	Yes	Yes	Yes	Yes
Acetone	C3H6O	235.0	46.9	Yes	Yes	Yes	Yes	Yes
Acetylene	C2H2	35.2	59.9	No	Yes	Yes	Yes	No
Ammonia (R-717)	NH3	132.4	113.6	Yes	Yes	Yes	Yes	Yes
Argon (R-740)	Ar	−122.5	48.6	Yes	Yes	Yes	Yes	Yes
Benzene	C6H6	288.9	49.1	Yes	Yes	Yes	Yes	Yes
Butane (R-600)	C4H10	152.0	38.0	Yes	Yes	Yes	Yes	Yes
Butene	C4H8	146.1	40.1	Yes	Yes	Yes	Yes	Yes
Carbon dioxide (R-744)	CO2	31.0	73.8	Yes	Yes	Yes	Yes	Yes
Carbon monoxide	CO	−140.3	34.9	Yes	Yes	Yes	Yes	Yes
Carbonyl sulfide	COS	105.6	63.7	No	Yes	Yes	Yes	No
Chlorine	Cl2	143.7	76.4	No	Yes	No	No	Yes
Chlorobenzene	C6H5Cl	359.2	45.2	No	Yes	No	Yes	Yes
cis-Butene	C4H8	162.6	42.3	Yes	Yes	Yes	Yes	Yes
Cyclobutene	C4H6	174.9	51.5	Yes	Yes	Yes	Yes	Yes
Cyclohexane	C6H12	280.5	40.8	Yes	Yes	Yes	Yes	Yes
Cyclopentane	C5H10	238.6	45.8	Yes	Yes	Yes	Yes	Yes
Cyclopropane	C3H6	125.2	55.8	Yes	Yes	Yes	Yes	Yes
D4	C8H24O4Si4	313.4	13.5	Yes	Yes	Yes	Yes	Yes
D5	C10H30O5Si5	345.2	10.9	Yes	Yes	Yes	Yes	Yes
D6	C12H36Si6O6	372.6	9.6	Yes	Yes	Yes	Yes	Yes
DEA	C4H11NO2	463.4	49.5	Yes	Yes	Yes	Yes	Yes
Decane	C10H22	344.6	21.0	Yes	Yes	Yes	Yes	Yes
Deuterium	D2	−234.8	16.8	Yes	Yes	Yes	Yes	Yes
Dichloroethane (R-150)	C2H4Cl2	288.5	52.3	No	Yes	No	Yes	Yes
Diethyl ether	C4H10O	193.6	37.2	No	Yes	Yes	Yes	No
Dimethyl carbonate	C3H6O3	283.9	49.1	Yes	Yes	Yes	Yes	Yes
Dimethyl ether (RE-170)	C2H6O	127.2	53.4	No	Yes	Yes	Yes	No
Docosane	C22H46	519.1	11.7	Yes	Yes	Yes	Yes	Yes
Dodecane	C12H26	385.0	18.2	Yes	Yes	Yes	Yes	Yes
Ethane (R-170)	C2H6	32.2	48.7	Yes	Yes	Yes	Yes	Yes
Ethanol	C2H6O	241.6	62.7	Yes	Yes	Yes	Yes	Yes
Ethylene glycol	C2H6O2	445.9	105.1	Yes	Yes	Yes	Yes	Yes
Ethylbenzene	C8H10	344.0	36.2	Yes	Yes	Yes	Yes	Yes
Ethylene (R-1150)	C2H4	9.2	50.4	No	Yes	Yes	Yes	No
Ethylene oxide	C2H4O	195.8	73.0	No	Yes	Yes	Yes	No
Fluorine	F2	−128.7	51.7	No	Yes	Yes	No	No
Heavy water	D2O	370.7	216.6	No	Yes	Yes	No	No
Helium (R-704)	He	−268.0	2.3	Yes	Yes	Yes	Yes	Yes
Heptane	C7H16	267.1	27.4	Yes	Yes	Yes	Yes	Yes
Hexadecane	C16H34	449.0	14.8	Yes	Yes	Yes	Yes	Yes
Hexane	C6H14	234.7	30.4	Yes	Yes	Yes	Yes	Yes
Hydrogen (R-702)	H2	−240.0	13.0	Yes	Yes	Yes	Yes	Yes
Hydrogen chloride	HCl	51.5	83.1	No	Yes	No	Yes	No
Hydrogen sulfide	H2S	100.0	90.0	No	Yes	Yes	No	Yes
Isobutane (R-600a)	C4H10	134.7	36.3	Yes	Yes	Yes	Yes	Yes
Isobutene	C4H8	144.9	40.1	No	Yes	Yes	Yes	No
Isohexane	C6H14	224.6	30.4	Yes	Yes	Yes	Yes	Yes
Isooctane	C8H18	270.9	25.7	Yes	Yes	Yes	Yes	Yes
Isopentane (R-601a)	C5H12	187.2	33.8	Yes	Yes	Yes	Yes	Yes
Krypton (R-784)	Kr	−63.7	55.3	Yes	Yes	Yes	Yes	Yes
MD2M	C10H30Si4O3	326.3	11.4	Yes	Yes	Yes	Unkown	Unkown
MD3M	C12H36Si5O4	355.8	9.6	Yes	Yes	Yes	Unkown	Unkown
MD4M	C14H42O5Si6	380.1	8.4	Yes	Yes	Yes	Unkown	Unkown
MDM	C8H24O2Si3	292.2	14.4	Yes	Yes	Yes	Unkown	Unkown
MEA	C2H7NO	398.3	81.3	Yes	Yes	Yes	Yes	Yes
Methane (R-50)	CH4	−82.6	46.0	Yes	Yes	Yes	Yes	Yes
Methanol	CH4O	240.2	82.2	Yes	Yes	Yes	Yes	Yes
Methyl linoleate	C19H34O2	525.9	13.4	Yes	Yes	Yes	Unkown	Unkown
Methyl linolenate	C19H32O2	498.9	13.7	Yes	Yes	Yes	Unkown	Unkown
Methyl oleate	C19H36O2	508.9	12.5	Yes	Yes	Yes	Unkown	Unkown
Methyl palmitate	C17H34O2	481.9	13.5	Yes	Yes	Yes	Unkown	Unkown
Methyl stearate	C19H38O2	501.9	12.4	Yes	Yes	Yes	Yes	Yes
Methylcyclohexane	C7H14	299.1	34.7	Yes	Yes	Yes	Yes	Yes
MM	C6H18OSi2	245.6	19.3	Yes	Yes	Yes	Unkown	Unkown
m-Xylene	C8H10	343.7	35.3	Yes	Yes	Yes	Yes	Yes
Neon(R-720)	Ne	−228.8	26.6	Yes	Yes	Yes	Unkown	Unkown
Neopentane	C5H12	160.6	32.0	Yes	Yes	Yes	Yes	Yes
Nitrogen (R-728)	N2	−147.0	34.0	Yes	Yes	Yes	Unkown	Unkown
Nitrogen trifluoride	F3N	−39.2	44.6	Yes	Yes	Yes	Unkown	Unkown
Nitrous oxide (R-744A)	N2O	36.4	72.5	No	No	Yes	Unkown	Unkown
Nonane	C9H20	321.4	22.8	Yes	Yes	Yes	Yes	Yes
Novec 649, 1230	C6F12O	168.7	18.7	Yes	Yes	Yes	Unkown	Unkown
Octane	C8H18	295.6	24.8	Yes	Yes	Yes	Yes	Yes
Orthohydrogen(R-702)	H2	−239.9	13.1	Yes	Yes	Yes	Yes	Yes
Oxygen (R-732)	O2	−118.6	50.4	Yes	Yes	Yes	Yes	Yes
o-Xylene	C8H10	357.1	37.4	Yes	Yes	Yes	Yes	Yes
Parahydrogen(R-702p)	H2	−240.2	12.9	Yes	Yes	Yes	Yes	Yes
Pentane (R-601)	C5H12	196.6	33.7	Yes	Yes	Yes	Yes	Yes
Perfluorobutane	C4F10	113.2	23.2	No	No	Yes	Unkown	Unkown
Perfluorohexane	C6F14	174.9	17.4	No	No	Yes	Unkown	Unkown
Perfluoropentane	C5F12	147.9	20.6	No	No	Yes	Unkown	Unkown
Propadiene	C3H4	124.9	52.2	Yes	Yes	Yes	Unkown	Unkown
Propane (R-290)	C3H8	96.7	42.5	Yes	Yes	Yes	Yes	Yes
Propylcyclohexane	C9H18	357.7	28.6	Yes	Yes	Yes	Unkown	Unkown
Propylene (R-1270)	C3H6	91.1	45.6	No	Yes	Yes	Yes	No

(*continued on next page*)

Table A.1 (*continued*).

Short name	Short formula	Critical temperature (°C)	Critical pressure (bar)	Passed working fluid screening?	GWP ≤ 150?	ODP ≈ 0?	NFPA health hazard ≤ 4?	NFPA Reactivity = 0?
Propylene oxide	C3H6O	215.0	54.4	No	Yes	Yes	Yes	No
Propyne	C3H4	129.2	56.3	No	Yes	Yes	Yes	No
p-Xylene	C8H10	343.0	35.3	Yes	Yes	Yes	Yes	Yes
R11	CCl3F	198.0	44.1	No	No	No	Unkown	Unkown
R1123	C2HF3	58.6	45.4	Yes	Yes	Yes	Unkown	Unkown
R113	C2Cl3F3	214.1	33.9	No	No	No	Unkown	Unkown
R114	C2Cl2F4	145.7	32.6	No	No	No	Yes	Yes
R115	C2ClF5	80.0	31.3	No	No	No	Yes	Yes
R116	C2F6	19.9	30.5	No	No	Yes	Yes	Yes
R12	CCl2F2	112.0	41.4	No	No	No	Yes	Yes
R1216	C3F6	85.8	31.5	No	Yes	Yes	Yes	No
R1224yd(Z)	C3HClF4	155.5	33.4	Yes	Yes	Yes	Yes	Yes
R123	C2HCl2F3	183.7	36.6	No	Yes	No	Yes	No
R1233zd(E)	C3H2ClF3	166.5	36.2	Yes	Yes	Yes	Yes	Yes
R1234yf	C3F4H2	94.7	33.8	Yes	Yes	Yes	Yes	Yes
R1234ze(E)	C3F4H2	109.4	36.3	Yes	Yes	Yes	Yes	Yes
R1234ze(Z)	C3F4H2	150.1	35.3	Yes	Yes	Yes	Yes	Yes
R124	C2HClF4	122.3	36.2	No	No	No	Unkown	Unkown
R1243zf	C3H3F3	103.8	35.2	Yes	Yes	Yes	Unkown	Unkown
R125	C2HF5	66.0	36.2	No	No	Yes	Unkown	Unkown
R13	CClF3	28.9	38.8	No	No	No	Unkown	Unkown
R1336mzz(Z)	C4H2F6	171.4	29.0	Yes	Yes	Yes	Yes	Yes
R134a	C2H2F4	101.1	40.6	No	No	Yes	Yes	No
R13I1	CF3I	123.3	39.5	No	Yes	No	Unkown	Unkown
R14	CF4	−45.6	37.5	No	No	Yes	Unkown	Unkown
R141b	C2H3Cl2F	204.4	42.1	No	No	No	Yes	Yes
R142b	C2H3ClF2	137.1	40.6	No	No	No	Yes	Yes
R143a	C2H3F3	72.7	37.6	No	No	Yes	Unkown	Unkown
R152a	C2H4F2	113.3	45.2	Yes	Yes	Yes	Unkown	Unkown
R161	C2H5F	102.1	50.5	Yes	Yes	Yes	Unkown	Unkown
R21	CHCl2F	178.3	51.8	No	No	No	Unkown	Unkown
R218	C3F8	71.9	26.4	No	No	Yes	Unkown	Unkown
R22	CHClF2	96.1	49.9	No	No	No	Yes	No
R227ea	C3HF7	101.8	29.3	No	No	Yes	Yes	No
R23	CHF3	26.1	48.3	No	No	Yes	Yes	Yes
R236ea	C3H2F6	139.3	34.2	No	No	Yes	Yes	Yes
R236fa	C3H2F6	124.9	32.0	No	No	Yes	Yes	Yes
R245ca	C3H3F5	174.4	39.4	No	No	Yes	Unkown	Unkown
R245fa	C3H3F5	153.9	36.5	No	No	Yes	Yes	Yes
R32	CH2F2	78.1	57.8	No	No	Yes	Yes	Yes
R365mfc	C4H5F5	186.9	32.7	No	No	No	Yes	Yes
R40	CH3Cl	143.2	66.9	No	Yes	No	Yes	Yes
R41	CH3F	44.1	59.0	Yes	Yes	Yes	Yes	Yes
RC318	C4F8	115.2	27.8	No	No	Yes	Unkown	Unkown
RE143a	C2H3F3O	104.8	36.4	No	No	Yes	Unkown	Unkown
RE245cb2	C3H3F5O	133.7	28.9	No	No	Yes	Unkown	Unkown
RE245fa2	C3H3F5O	171.7	34.3	No	No	Yes	Unkown	Unkown
RE347mcc (HFE-7000)	C4H3F7O	164.6	24.8	No	No	Yes	Unkown	Unkown
Sulfur dioxide (R-764)	O2S	157.5	78.9	Yes	Yes	Yes	Yes	Yes
Sulfur hexafluoride	SF6	45.6	37.5	No	No	Yes	Unkown	Unkown
Toluene	C7H8	318.6	41.3	Yes	Yes	Yes	Yes	Yes
trans-Butene	C4H8	155.5	40.3	No	Yes	Yes	Yes	No
Undecane	C11H24	365.7	19.9	Yes	Yes	Yes	Yes	Yes
Vinyl chloride (R-1140)	C2H3Cl	151.8	55.9	No	Yes	No	Yes	No
Water (R-718)	H2O	373.9	220.6	Yes	Yes	Yes	Yes	Yes
Xenon	Xe	16.6	58.4	Yes	Yes	Yes	Unkown	Unkown

References

[1] International Energy Agency (IEA), Net zero by 2050, 2021, https://www.iea.org/reports/net-zero-by-2050.

[2] A. Marina, S. Spoelstra, H. Zondag, A. Wemmers, An estimation of the European industrial heat pump market potential, Renew. Sustain. Energy Rev. 139 (2021) 110545.

[3] J. Jiang, B. Hu, R. Wang, N. Deng, F. Cao, C.-C. Wang, A review and perspective on industry high-temperature heat pumps, Renew. Sustain. Energy Rev. 161 (2022) 112106.

[4] C. Arpagaus, F. Bless, M. Uhlmann, J. Schiffmann, S.S. Bertsch, High temperature heat pumps: Market overview, state of the art, research status, refrigerants, and application potentials, Energy 152 (2018) 985–1010.

[5] O. Bamigbetan, T.M. Eikevik, P. Nekså, M. Bantle, Review of vapour compression heat pumps for high temperature heating using natural working fluids, Int. J. Refrig. 80 (2017) 197–211.

[6] K.-M. Adamson, T.G. Walmsley, J.K. Carson, Q. Chen, F. Schlosser, L. Kong, D.J. Cleland, High-temperature and transcritical heat pump cycles and advancements: A review, Renew. Sustain. Energy Rev. 167 (2022) 112798.

[7] R. Bergamini, J.K. Jensen, B. Elmegaard, Thermodynamic competitiveness of high temperature vapor compression heat pumps for boiler substitution, Energy 182 (2019) 110–121.

[8] M. Jesper, F. Schlosser, F. Pag, T.G. Walmsley, B. Schmitt, K. Vajen, Large-scale heat pumps: Uptake and performance modelling of market-available devices, Renew. Sustain. Energy Rev. 137 (2021) 110646.

[9] R. de Boer, A. Marina, B. Zühlsdorf, C. Arpagaus, M. Bantle, V. Wilk, B. Elmegaard, J. Corberán, J. Benson, Strengthening industrial heat pump innovation: Decarbonizing industrial heat, 2020.

[10] B. Hu, D. Wu, L. Wang, R. Wang, Exergy analysis of R1234ze(Z) as high temperature heat pump working fluid with multi-stage compression, Front. Energy 11 (2017) 493–502.

[11] B. Zühlsdorf, J.K. Jensen, S. Cignitti, C. Madsen, B. Elmegaard, Analysis of temperature glide matching of heat pumps with zeotropic working fluid mixtures for different temperature glides, Energy 153 (2018) 650–660.

[12] C. Xu, H. Yang, X. Yu, H. Ma, M. Chen, M. Yang, Performance analysis for binary mixtures based on R245fa using in high temperature heat pumps, Energy Convers. Manag.: X 12 (2021) 100123.

[13] W. Xu, R. Zhao, S. Deng, L. Zhao, S.S. Mao, Is zeotropic working fluid a promising option for organic rankine cycle: A quantitative evaluation based on literature data, Renew. Sustain. Energy Rev. 148 (2021) 111267.

[14] H. Abedini, E. Vieren, T. Demeester, W. Beyne, S. Lecompte, S. Quoilin, A. Arteconi, A comprehensive analysis of binary mixtures as working fluid in high temperature heat pumps, Energy Convers. Manage. 277 (2023) 116652.

[15] G. Bamorovat Abadi, K.C. Kim, Investigation of organic rankine cycles with zeotropic mixtures as a working fluid: Advantages and issues, Renew. Sustain. Energy Rev. 73 (2017) 1000–1013.

[16] S. Lecompte, B. Ameel, D. Ziviani, M. van den Broek, M. De Paepe, Exergy analysis of zeotropic mixtures as working fluids in organic rankine cycles, Energy Convers. Manage. 85 (2014) 727–739.

[17] F. Heberle, M. Preißinger, D. Brüggemann, Zeotropic mixtures as working fluids in organic rankine cycles for low-enthalpy geothermal resources, Renew. Energy 37 (1) (2012) 364–370.

[18] M. Chys, M. van den Broek, B. Vanslambrouck, M. De Paepe, Potential of zeotropic mixtures as working fluids in organic rankine cycles, Energy 44 (1) (2012) 623–632, Integration and Energy System Engineering, European Symposium on Computer-Aided Process Engineering 2011.

[19] G. Lorentzen, Trans-critical vapour compression cycle device, 1990, Google Patents.

[20] G. Lorentzen, Revival of carbon dioxide as a refrigerant, Int. J. Refrig. 17 (5) (1994) 292–301.

[21] B.T. Austin, K. Sumathy, Transcritical carbon dioxide heat pump systems: A review, Renew. Sustain. Energy Rev. 15 (8) (2011) 4013–4029.

[22] R.U. Rony, H. Yang, S. Krishnan, J. Song, Recent advances in transcritical CO2 (R744) heat pump system: A review, Energies 12 (3) (2019).

[23] D. Yang, Y. Li, J. Xie, J. Wang, Research and application progress of transcritical CO2 refrigeration cycle system: A review, Int. J. Low-Carbon Technol. 17 (2021) 245–256.

[24] Y. Ma, Z. Liu, H. Tian, A review of transcritical carbon dioxide heat pump and refrigeration cycles, Energy 55 (2013) 156–172.

[25] M.-H. Kim, J. Pettersen, C. Bullard, Fundamental process and system design issues in CO2 vapor compression systems, Prog. Energy Combust. Sci. 30 (2004) 119–174.

[26] S. Lecompte, E. Ntavou, B. Tchanche, G. Kosmadakis, A. Pillai, D. Manolakos, M. De Paepe, Review of experimental research on supercritical and transcritical thermodynamic cycles designed for heat recovery application, Appl. Sci. 9 (2019) 2571.

[27] J. Sarkar, S. Bhattacharyya, M. Ram Gopal, Natural refrigerant-based subcritical and transcritical cycles for high temperature heating, Int. J. Refrig. 30 (1) (2007) 3–10.

[28] K. Besbes, A. Zoughaib, F. Carlan, J.-L. Peureux, A R-32 transcritical heat pump for high temperature industrial applications, in: Proceedings of the 24th IIR International Congress of Refrigeration, ICR2015, 2015.

[29] G. Abi Chahla, Y. Beucher, A. Zoughaib, F. Carlan, J. Pierrucci, Transcritical industrial heat pump using HFO's for up to 150°C hot air supply, in: Proceedings of the 25th IIR International Congress of Refrigeration, ICR2019, 2019.

[30] T. Kimura, H. Fuchikami, K. Nishida, M. Kuda, A. Macida, K. Saito, Y. Ohta, M. Katsuta, Proceedings of the JRAIA International Symposium 2018, JRAIA2018.

[31] M. Verdnik, R. Rieberer, Influence of operating parameters on the COP of an R600 high-temperature heat pump, Int. J. Refrig. 140 (2022) 103–111.

[32] J. Wang, C. Brown, D. Cleland, Heat pump heat recovery options for food industry dryers, Int. J. Refrig. 86 (2018) 48–55.

[33] C. Arpagaus, F. Bless, S. Bertsch, Theoretical analysis of transcritical HTHP cycles with low gwp hfo refrigerants and hydrocarbons for process heat up to 200 °C, in: Proceedings of the IIR Rankine Conference, IIR, 2020.

[34] E.W. Lemmon, I.H. Bell, M.L. Huber, M.O. McLinden, NIST Standard Reference Database 23: Reference Fluid Thermodynamic and Transport Properties-REFPROP, Version 10.0, National Institute of Standards and Technology, 2018.

[35] P.A. Domanski, J. Steven Brown, J. Heo, J. Wojtusiak, M.O. McLinden, A thermodynamic analysis of refrigerants: Performance limits of the vapor compression cycle, Int. J. Refrig. 38 (2014) 71–79.

[36] B. Saleh, M. Wendland, Screening of pure fluids as alternative refrigerants, Int. J. Refrig. 29 (2) (2006) 260–269.

[37] D. Calleja-Anta, L. Nebot-Andrés, J. Catalán-Gil, D. Sánchez, R. Cabello, R. Llopis, Thermodynamic screening of alternative refrigerants for R290 and R600a, Results Eng. 5 (2020) 100081.

[38] P. Domanski, J. Brown, E. Lemmon, CYCLE D: NIST Vapor Compression Cycle Design Program, Version 6.0; User's Guide, Natl Std. Ref. Data Series (NIST NSRDS), National Institute of Standards and Technology, Gaithersburg, MD, 2018.

[39] M. Pitarch, E. Hervas-Blasco, E. Navarro-Peris, J. Gonzálvez-Maciá, J.M. Corberán, Evaluation of optimal subcooling in subcritical heat pump systems, Int. J. Refrig. 78 (2017) 18–31.

[40] B. Zühlsdorf, F. Bühler, M. Bantle, B. Elmegaard, Analysis of technologies and potentials for heat pump-based process heat supply above 150 °C, Energy Convers. Manag.: X 2 (2019) 100011.

[41] G. Kosmadakis, P. Neofytou, Investigating the effect of nanorefrigerants on a heat pump performance and cost-effectiveness, Therm. Sci. Eng. Prog. 13 (2019) 100371.

[42] C. Mateu-Royo, J. Navarro-Esbrí, A. Mota-Babiloni, F. Molés, M. Amat-Albuixech, Experimental exergy and energy analysis of a novel high-temperature heat pump with scroll compressor for waste heat recovery, Appl. Energy 253 (2019) 113504.

[43] G. Kosmadakis, C. Arpagaus, P. Neofytou, S. Bertsch, Techno-economic analysis of high-temperature heat pumps with low-global warming potential refrigerants for upgrading waste heat up to 150 °C, Energy Convers. Manage. 226 (2020) 113488.

[44] M. Astolfi, Techno-economic optimization of low temperature CSP systems based on ORC with screw expanders, Energy Procedia 69 (2015) 1100–1112, International Conference on Concentrating Solar Power and Chemical Energy Systems, SolarPACES 2014.

[45] M. Yang, T. Li, X. Feng, Y. Wang, A simulation-based targeting method for heat pump placements in heat exchanger networks, Energy 203 (2020) 117907.

[46] C. Kondou, S. Koyama, Thermodynamic assessment of high-temperature heat pumps using Low-GWP HFO refrigerants for heat recovery, Int. J. Refrig. 53 (2015) 126–141.

[47] C. Underwood, 14 - Heat pump modelling, in: S.J. Rees (Ed.), Advances in Ground-Source Heat Pump Systems, Woodhead Publishing, 2016, pp. 387–421.

[48] B. Luo, P. Zou, Performance analysis of different single stage advanced vapor compression cycles and refrigerants for high temperature heat pumps, Int. J. Refrig. 104 (2019) 246–258.

[49] G.F. Frate, L. Ferrari, U. Desideri, Analysis of suitability ranges of high temperature heat pump working fluids, Appl. Therm. Eng. 150 (2019) 628–640.

[50] C. Mateu-Royo, J.N.-E.A. Mota-Babiloni, M. Amat-Albuixech, F. Molés, Theoretical evaluation of different high-temperature heat pump configurations for low-grade waste heat recovery, Int. J. Refrig. 90 (2018) 229–237.

[51] O. Ibrahim, F. Fardoun, R. Younes, H. Louahlia-Gualous, Air source heat pump water heater: Dynamic modeling, optimal energy management and mini-tubes condensers, Energy 64 (2014) 1102–1116.

[52] J. Van Nieuwenhuyse, S. Lecompte, M. De Paepe, Current status of the thermo-hydraulic behavior of supercritical refrigerants: A review, Appl. Therm. Eng. 218 (2023) 119201.

[53] T. Deethayat, T. Kiatsiriroat, C. Thawonngamyingsakul, Performance analysis of an organic rankine cycle with internal heat exchanger having zeotropic working fluid, Case Stud. Therm. Eng. 6 (2015) 155–161.

[54] Z. Zhang, L. Tian, Y. Chen, L. Tong, Effect of an internal heat exchanger on performance of the transcritical carbon dioxide refrigeration cycle with an expander, Entropy 16 (11) (2014) 5919–5934.

[55] K. Yang, Y. Zhang, X. Li, J. Xu, Theoretical evaluation on the impact of heat exchanger in advanced adiabatic compressed air energy storage system, Energy Convers. Manage. 86 (2014) 1031–1044.

[56] Y. Wang, Z. Ye, X. Yin, Y. Song, F. Cao, Energy, exergy and exergoeconomic evaluation of the air source transcritical CO2 heat pump with internal heat exchanger for space heating, Int. J. Refrig. 130 (2021) 14–26.

[57] V. Pérez-García, A. Mota-Babiloni, J. Navarro-Esbrí, Influence of operational modes of the internal heat exchanger in an experimental installation using R-450a and R-513A as replacement alternatives for R-134a, Energy 189 (2019) 116348.

[58] N. Zheng, L. Zhao, The feasibility of using vapor expander to recover the expansion work in two-stage heat pumps with a large temperature lift, Int. J. Refrig. 56 (2015) 15–27.

[59] G. Ferrara, L. Ferrari, D. Fiaschi, G. Galoppi, S. Karellas, R. Secchi, D. Tempesti, A small power recovery expander for heat pump COP improvement, Energy Procedia 81 (2015) 1151–1159, 69th Conference of the Italian Thermal Engineering Association, ATI 2014.

[60] J. Sarkar, Ejector enhanced vapor compression refrigeration and heat pump systems—A review, Renew. Sustain. Energy Rev. 16 (9) (2012) 6647–6659.

[61] X. Chen, S. Omer, M. Worall, S. Riffat, Recent developments in ejector refrigeration technologies, Renew. Sustain. Energy Rev. 19 (2013) 629–651.

[62] B. Zühlsdorf, F. Bühler, R. Mancini, S. Cignitti, B. Elmegaard, High temperature heat pump integration using zeotropic working fluids for spray drying facilities, in: Proceedings of the 12th IEA Heat Pump Conference 2017, 2017, 12th IEA Heat Pump Conference ; Conference date: 15-05-2017 Through 18-05-2017.

[63] D. Mikielewicz, J. Wajs, Performance of the very high-temperature heat pump with low GWP working fluids, Energy 182 (2019) 460–470.

[64] H. Yan, L. Ding, B. Sheng, X. Dong, Y. Zhao, Q. Zhong, W. Gong, M. Gong, H. Guo, J. Shen, Performance prediction of HFC, HC, HFO and HCFO working fluids for high temperature water source heat pumps, Appl. Therm. Eng. 185 (2021) 116324.

[65] P. Virtanen, R. Gommers, T.E. Oliphant, M. Haberland, T. Reddy, D. Cournapeau, E. Burovski, P. Peterson, W. Weckesser, J. Bright, S.J. van der Walt, M. Brett, J. Wilson, K.J. Millman, N. Mayorov, A.R.J. Nelson, E. Jones, R. Kern, E. Larson, C.J. Carey, İ. Polat, Y. Feng, E.W. Moore, J. VanderPlas, D. Laxalde, J. Perktold, R. Cimrman, I. Henriksen, E.A. Quintero, C.R. Harris, A.M. Archibald, A.H. Ribeiro, F. Pedregosa, P. van Mulbregt, SciPy 1.0 Contributors, SciPy 1.0: Fundamental algorithms for scientific computing in Python, Nature Methods 17 (2020) 261–272.

[66] European Parliament, Regulation (EU) no 517/2014 of the European parliament and of the council of 16 april 2014 on fluorinated greenhouse gases and repealing regulation (EC) no 842/2006, 2014, https://eur-lex.europa.eu/eli/reg/2014/517/oj (Accessed: 08 April 2021).

[67] European Parliament, Regulation (EC) no 1005/2009 of the European parliament and of the council of 16 september 2009 on substances that deplete the ozone layer, 2009, https://eur-lex.europa.eu/legal-content/EN/TXT/?uri=CELEX:32009R1005j (Accessed: 08 April 2021).

[68] National Fire Protection Association (NFPA), NFPA 704: Standard system for the identification of the hazards of materials for emergency response, 2022, https://www.nfpa.org/codes-and-standards/all-codes-and-standards/list-of-codes-and-standards/detail?code=704 (Accessed: 07 July 2022).

[69] X. Dai, L. Shi, Q. An, W. Qian, Chemical kinetics method for evaluating the thermal stability of organic rankine cycle working fluids, Appl. Therm. Eng. 100 (2016) 708–713.

[70] W.C. Andersen, T.J. Bruno, Rapid screening of fluids for chemical stability in organic rankine cycle applications, Ind. Eng. Chem. Res. 44 (15) (2005) 5560–5566.

[71] K. Harby, Hydrocarbons and their mixtures as alternatives to environmental unfriendly halogenated refrigerants: An updated overview, Renew. Sustain. Energy Rev. 73 (2017) 1247–1264.

[72] E. Granryd, Hydrocarbons as refrigerants — an overview, Int. J. Refrig. 24 (1) (2001) 15–24.

[73] O. Bamigbetan, T.M. Eikevik, P. Nekså, M. Bantle, C. Schlemminger, Experimental investigation of a prototype R-600 compressor for high temperature heat pump, Energy 169 (2019) 730–738.

[74] International Energy Agency (IEA); Heat Pump Technologies (HPT), Annex58 task 1: Technologies – state of the art and ongoing developments for systems and components, 2022, https://heatpumpingtechnologies.org/annex58/task1/ (Accessed: 12 Apri 2023).
[75] J. Galindo, S. Ruiz, V. Dolz, L. Royo-Pascual, R. Haller, B. Nicolas, Y. Glavatskaya, Experimental and thermodynamic analysis of a bottoming organic rankine cycle (ORC) of gasoline engine using swash-plate expander, Energy Convers. Manage. 103 (2015) 519–532.
[76] P. Colonna, E. Casati, C. Trapp, T. Mathijssen, J. Larjola, T. Turunen-Saaresti, A. Uusitalo, Organic Rankine Cycle Power Systems: From the Concept to Current Technology, Applications, and an Outlook to the Future, J. Eng. Gas Turbines Power 137 (10) (2015) 100801.
[77] The American Society of Heating, Refrigerating and Air-Conditioning Engineers (ASHRAE), ASHRAE 34 refrigerant designations, 2022, https://www.ashrae.org/technical-resources/standards-and-guidelines/ashrae-refrigerant-designations (Accessed: 07 July 2022).
[78] M. Yang, B. Wang, X. Li, W. Shi, L. Zhang, Evaluation of two-phase suction, liquid injection and two-phase injection for decreasing the discharge temperature of the R32 scroll compressor, Int. J. Refrig. 59 (2015) 269–280.
[79] X.-Q. Cao, W.-W. Yang, F. Zhou, Y.-L. He, Performance analysis of different high-temperature heat pump systems for low-grade waste heat recovery, Appl. Therm. Eng. 71 (1) (2014) 291–300.
[80] Bitzer, Bitzer products, 2022, https://www.bitzer.de/gb/en/products/ (Accessed: 07 July 2022).
[81] Frascold, Frascold products, 2022, https://www.frascold.it/en/product-search?s=9 (Accessed: 07 July 2022).
[82] Emerson Copeland, Emerson copeland, 2022, https://climate.emerson.com/en-us/brands/copeland (Accessed: 07 July 2022).
[83] SRMtec, Srmtec compressors, 2022, https://srmtec.it/en/ (Accessed: 07 July 2022).
[84] T. Ommen, J.K. Jensen, W.B. Markussen, L. Reinholdt, B. Elmegaard, Technical and economic working domains of industrial heat pumps: Part 1 – single stage vapour compression heat pumps, Int. J. Refrig. 55 (2015) 168–182.
[85] Bock, Bock products, 2022.
[86] M.H. Bade, S. Bandyopadhyay, Minimization of thermal oil flow rate for indirect integration of multiple plants, Ind. Eng. Chem. Res. 53 (33) (2014) 13146–13156.
[87] N. Hampel, K.H. Le, A. Kharaghani, E. Tsotsas, Continuous modeling of superheated steam drying of single rice grains, Drying Technol. 37 (12) (2019) 1583–1596.
[88] H. Romdhana, C. Bonazzi, M. Esteban-Decloux, Superheated steam drying: An overview of pilot and industrial dryers with a focus on energy efficiency, Drying Technol. 33 (10) (2015) 1255–1274.
[89] C. Bang-Møller, M. Rokni, B. Elmegaard, J. Ahrenfeldt, U. Henriksen, Decentralized combined heat and power production by two-stage biomass gasification and solid oxide fuel cells, Energy 58 (2013) 527–537.
[90] C. Arpagaus, S. Bertsch, Experimental Comparison of HCFO and HFO R1224yd(Z), R1233zd(E), R1336mzz(Z), and HFC R245fa in a High Temperature Heat Pump up to 150 °C Supply Temperature, in: Proceedings of the 18th International Refrigeration and Air Conditioning Conference, IRACC2021, Purdue, US, 2021.
[91] DryFiciency (Dry-F), DryFiciency web page, 2022, https://dryficiency.eu/ (Accessed: 08 Dec 2022).